

# Scanning Microscopy

---

Volume 10 | Number 3

Article 4

---

3-20-1996

## Experimental Measurements of Electron Stopping Power at Low Energies

David C. Joy

*University of Tennessee*, [djoy@utk.edu](mailto:djoy@utk.edu)

Suichu Luo

*University of Tennessee*

Raynald Gauvin

*University de Sherbrooke*


Pierre Hovington

*University de Sherbrooke*

Neal Evans

*Oak Ridge Institute for Science and Engineering*

Follow this and additional works at: <https://digitalcommons.usu.edu/microscopy>

 Part of the [Biology Commons](#)

---

### Recommended Citation

Joy, David C.; Luo, Suichu; Gauvin, Raynald; Hovington, Pierre; and Evans, Neal (1996) "Experimental Measurements of Electron Stopping Power at Low Energies," *Scanning Microscopy*. Vol. 10 : No. 3 , Article 4.

Available at: <https://digitalcommons.usu.edu/microscopy/vol10/iss3/4>

This Article is brought to you for free and open access by the Western Dairy Center at DigitalCommons@USU. It has been accepted for inclusion in Scanning Microscopy by an authorized administrator of DigitalCommons@USU. For more information, please contact [digitalcommons@usu.edu](mailto:digitalcommons@usu.edu).



## EXPERIMENTAL MEASUREMENTS OF ELECTRON STOPPING POWER AT LOW ENERGIES

David C. Joy\*, Suichu Luo, Raynald Gauvin<sup>1</sup>, Pierre Hovington<sup>1</sup> and Neal Evans<sup>2</sup>

EM Facility, University of Tennessee, Knoxville, TN 37996-0810  
and Oak Ridge National Laboratory, Oak Ridge TN 37996

<sup>1</sup>Dépt. de génie mécanique, Univ. de Sherbrooke, Sherbrooke, PQ, Canada J1K 2R1

<sup>2</sup>Oak Ridge Institute for Science and Engineering, PO Box 117, Oak Ridge, TN 37831-0117

(Received for publication December 2, 1995 and in revised form March 20, 1996)

### Abstract

The electron stopping power has been measured for twelve elements and fifteen compounds, over the energy range from 1 eV to 10 keV, by the analysis of electron energy loss spectra, optical data, and photon mass absorption data. Values of the effective mean ionization potential  $J_{\text{eff}}$  and the effective number of participating electrons  $N_{\text{eff}}$  have also been determined in each case. The results obtained have been compared with other experimental data, with first-principles theoretical calculations, and with a number of proposed analytical models.

**Key Words:** Electron stopping power, mean ionization potential, Bethe range, electron spectroscopy.

### Introduction

Electron stopping power is the rate (in eV/Å) at which an electron transfers its energy to the material through which it is traveling. A knowledge of this quantity is an essential requirement in the understanding and modeling of electron-solid interactions, since it determines not only the range of the electrons in the solid, but also the extent of their lateral scattering, and the spatial distribution and magnitude of the X-ray, secondary electron, and electron-hole pair production (Nieminen, 1988). An accurate knowledge of stopping powers at low energies, here defined as 10 keV and below, is now particularly important because of the widespread use of low energy electron beams for technologies such as electron lithography and critical dimension metrology.

### A Simple Theory of Electron Stopping Power

Bethe's (1930) classic paper on electron-solid interactions, based on an earlier theoretical study by Thompson (1912), gave the stopping power of the electron in the form:

$$-\frac{dE}{dx} = \frac{4\pi NZe^4\rho}{m_0v^2A} \ln \left[ \frac{m_0v^2}{J} \right] \quad (1)$$

where  $N$  is Avogadro's number,  $Z$  and  $A$  are respectively the atomic number and the atomic weight of the atom,  $\rho$  is the density of the target,  $e$  and  $m_0$  are the charge and the rest mass of the electron,  $v$  is the electron velocity. The Bethe stopping power relationship has the significant advantage that only one parameter  $J$ , the mean ionization potential, is required to define the behavior of the material over the entire energy range. The value of  $J$  represents a sum over all inelastic excitations that the electron can produce, so the magnitude of  $J$  will only be constant at energies that are high enough to permit all possible excitations. At lower energies, some events,

\*Address for correspondence:

David C Joy  
F239, Walters Life Science Building  
University of Tennessee  
Knoxville, TN 37996-0810

Telephone number: 423-974-3642

FAX number: 423-974-9449

E-mail: djoy@utk.edu

e.g., inner shell ionizations, will no longer be allowed and so the value of  $J$  will fall. In the limit where  $J$  is changing,  $Z$  will also change because not all of the electrons associated with the atom will be excited. The problem with calculating electron stopping power at low energy is, therefore, to determine appropriate values for  $J$  and  $Z$  as a function of electron energy.

### Techniques for the Determination of Stopping Power at Low Energies

A computation of the electron stopping power in the energy range below 10 keV can be made in several different ways. The most common approach has been to assume that eq. (1) is correct and complete and to use it for a direct calculation. This in turn requires a value for  $J$ , and extensive tabulations for elements and selected compounds are available (ICRU, 1984). The values supplied in those tables have been determined from measurements of the energy loss, or penetration, of high energy (several MeV) protons and alpha-particles, and so represent the limiting high energy maximum value of  $J$  (Berger and Seltzer, 1982). Stopping powers computed using these  $J$  values have been very widely used in electron microscopy and microanalysis and have generally been found to be satisfactory for incident energies in excess of about 10 keV (Berger and Seltzer, 1982). However, at lower energies, it is often found desirable to modify particular  $J$  values in order to achieve the highest accuracies in the quantification of electron probe microanalysis data (e.g., Duncumb and Da Casa, 1969; Pouchou and Pichoir, 1987). For example, Harrowfield *et al.*, (1994) have demonstrated how the detailed shape of the X-ray continuum from a solid can be used to test and refine stopping power models and to determine optimum values for mean ionization potentials  $J$  at lower beam energies.

Alternatively, Flinn and Salehi (1980) have suggested that if the variation of secondary electron yield  $\delta$  as a function of energy  $E$  were regarded as the measure of an effective cross-section  $\sigma_{SE}$ , then a Fano plot of  $\sigma_{SE} \cdot E$  against  $\ln(E)$  would yield a straight line with an intercept of  $\ln(J)$ , hence yielding an appropriate low energy value for the mean ionization potential. Their application of this method to mixed oxide materials, and tests of this method on other published SE yield curves (e.g., data in Joy, 1995) mostly confirm that the Fano plot is linear, but the  $J$  values derived from this analysis have poor accuracy and precision compared to values obtained by more conventional techniques.

For low energies, improved agreement between first principles calculations of stopping power (Ashley *et al.*, 1979; Tung *et al.*, 1979) and the standard Bethe expression can be obtained by accounting for the fact that the mean ionization potential falls as the electron energy is

reduced. Livingstone and Bethe (1937) separated eq. (1) into two components characterized by different  $J$  values, one representing the contribution to the stopping power from the K-shell, and the other the contribution from all of the other electrons. At high energies, the combined expression is evaluated and is identical to the original Bethe expression, but at low energies ( $E < 1.5E_{crit}$ , where  $E_{crit}$  is the critical energy for ionization of the K-shell), only the second term is evaluated. This approach has recently been further developed by Brizuela and Riveros (1990) and is discussed below.

An empirical approach has been suggested by Joy and Luo (1989), who rewrote eq. (1) in the form:

$$-\frac{dE}{dx} = \frac{4\pi N e^4 \rho Z}{m_0 v^2 A} \ln \left[ \frac{1.166(E + kJ)}{J} \right] \quad (2)$$

where  $k$  is a constant with a value of about 0.85. This modified equation tends to the standard Bethe expression at high energies, but at low energies has the effect of making  $J$  effectively a function of  $E$  and also removes the problem in evaluating eq. (1) when  $E \leq J$ . When compared with first-principles calculations (e.g., Tung *et al.*, 1979), this procedure results in a considerable gain in accuracy.

The stopping power can also be determined directly from suitable experiments. Garber *et al.* (1971) studied the transmission of low energy electrons through thin foils of aluminum placed on an oxide insulator and supported on top of a conductor strip and showed that the stopping power could be determined from an analysis of the electron currents recorded from different portions of the structure. While the analysis of the data was not straightforward, and required careful corrections for secondary electron yield effects, reproducible values were obtained which were in good agreement with values estimated from the Bethe equation.

Stopping powers may also be experimentally determined by calorimetry. Al-Ahmad and Watt (1983) have obtained stopping power data for several metals by measuring the temperature rise of thin foils exposed to an electron beam of various energies between 1 and 10 keV. Although the analysis of the data requires some approximations, the values they obtained are in good agreement with other determinations and provide a useful, independent, check. Assessments of the total thermal energy deposition of higher energy beams in thin foils have also been reported by Rez and Glaisher (1991).

The most powerful techniques for determining stopping powers involve the use of spectroscopic methods. For example, direct measurements of mean energy

losses from electron energy loss spectroscopy have been used by Ishigure *et al.* (1978) to find the stopping power in aluminum. More generally (for good reviews, see Daniels *et al.*, 1970; and Ashley, 1988), optical or electron spectroscopy can be employed to determine the complex dielectric function  $\epsilon(q, \omega)$ , at a frequency  $\omega$  and momentum-transfer  $q$ , for a material of interest. From an application of the Kramers-Kronig transform, the real and imaginary parts of  $\epsilon(q, \omega)$  can then be determined and the stopping power computed directly (e.g., Ashley, 1988). Although optical spectroscopy has been widely used for this purpose, electron spectroscopy has the merit of allowing non-zero  $q$  vectors to be explored, and adds the practical advantage that measurements can be obtained from very small amounts of a material by performing the spectroscopy in a transmission electron microscope.

### Experimental Technique

The technique used for the results reported here uses electron energy loss spectroscopy to determine the complex dielectric coefficient  $\epsilon(q, \omega)$  and then computes the stopping power from that quantity. The method used (Luo *et al.*, 1991) is that of Ritchie and Howie (1977), who showed that the potential due to an electron moving with a velocity  $v$  in a uniform, infinite, dielectric medium satisfies the equation:

$$\epsilon_0 \cdot \epsilon(q, \omega) \cdot \nabla^2 \varphi(r, t) = e \delta(r - vt) \quad (3)$$

where  $\epsilon(q, \omega)$  is the dielectric function,  $q$  is the wave vector, and  $\hbar q$  and  $\hbar \omega$  are respectively the momentum transfer and energy transfer to the electrons in the solid. In Fourier space,

$$\varphi(q, \omega) = -\frac{2\pi e \delta(q \cdot v + \omega)}{\epsilon_0 \cdot \epsilon(q, \omega) \cdot q^2} \quad (4)$$

and where

$$\varphi(r, t) = \frac{1}{(2\pi)^4} \int dq \int d\omega \cdot \exp[i(q \cdot r + \omega t)] \cdot \varphi(q, \omega) \quad (5)$$

The stopping power  $dE/ds$  along a segment of the electron trajectory of length  $s$  is then

$$-\frac{dE}{ds} = e(-\nabla \varphi(r, t)) \cdot s \quad (6)$$

which, if  $\phi$  is expressed in terms of its Fourier representation, can be written as

$$-\frac{dE}{ds} = \frac{h^2}{4\pi^3 a_0 E_T} \cdot \int \int q_p \omega \operatorname{Im} \left[ -\frac{1}{\epsilon(q, \omega)} \right] \cdot \frac{dq_p d\omega}{q_p^2 + (\omega/v)^2} \quad (7)$$

where  $a_0$  is the Bohr radius,  $q_p$  is the component of  $q$  in the direction perpendicular to  $v$ , and for an electron of energy  $E$

$$E_T = E \cdot \frac{(1 + E/1022)}{(1 + E/511)^2}$$

The stopping power can also be defined from the inelastic scattering cross-section  $\sigma$  as

$$-\frac{dE}{ds} = \int \int nE \frac{d^2\sigma}{d\Omega \cdot dE} d\Omega \cdot dE \quad (8)$$

where  $n$  is the number of atoms or molecules per unit volume of the sample. Equating eqs. (7) and (8) then gives the differential cross-section

$$\frac{d^2\sigma}{d\Omega \cdot dE} = \frac{1}{2\pi^2 a_0 n E_T} \operatorname{Im} \left[ -\frac{1}{\epsilon(q, \omega)} \right] \left[ \frac{1}{\theta^2 + \theta_E^2} \right] \quad (9)$$

where  $\theta$  is the scattering angle,  $d\Omega = 2\pi \theta d\theta$ ,  $\theta_E = E/(2\gamma E_T)$ ,  $\gamma^2 = 1/(1 - \beta^2)$  and  $\beta = v/c$  where  $c$  is the speed of light.

In the ideal case, the measured energy loss spectrum represents the single scattering distribution  $S(E)$ , i.e., the distribution of transmitted electrons which have suffered at most only a single inelastic event.  $S(E)$  can be written (Egerton, 1996) as

$$S(E) = I_0 \left[ \frac{\rho t N}{A} \right] \left[ \frac{d\sigma}{dE} \right] \quad (10)$$

where  $I_0$  is the incident beam current. If it can be assumed that  $\operatorname{Im}[-1/\epsilon(q, \omega)]$  is independent of the scattering angle  $\theta$  within the angular range of collection, then from eqs. (9) and (10),

$$S(E) = \frac{I_0 t}{2\pi a_0 E_T} \text{Im} \left[ -\frac{1}{\epsilon(q, \omega)} \right] \cdot \ln \left[ 1 + \left( \frac{\alpha}{\theta_E} \right)^2 \right] \quad (11)$$

where  $\alpha$  is the semi-angle of collection for the spectrum. The imaginary part of the dielectric function can thus be determined from an electron energy loss (EELS) experiment. Because  $\epsilon(q, \omega)$  satisfies the sum-rule

$$Z = \frac{\epsilon_0 M_0}{(\pi/2) e^2 n} \int_0^\infty \omega \cdot \text{Im} \left[ -\frac{1}{\epsilon(q, \omega)} \right] d\omega \quad (12)$$

it is not necessary to know the thickness  $t$  of the specimen from which the spectrum was obtained in order to obtain the absolute magnitude of  $\text{Im} [-1/\epsilon]$ .

The Kramers-Kronig transform (Egerton, 1996) is then applied to obtain  $\text{Re} (\epsilon(E))$  the real part of the dielectric function, and the real and imaginary parts are then normalized from the sum rule:

$$1 - \text{Re} \left[ \frac{1}{\epsilon(0)} \right] = \frac{2}{\pi} \int_0^\infty \text{Im} \left[ -\frac{1}{\epsilon(E)} \right] \frac{dE}{E} \quad (13)$$

For a metal, the left hand side of eq. (13) is unity, while for an insulator,  $\text{Re} [1/\epsilon(0)]$  is just  $1/\epsilon_1(0)$ , where  $\epsilon_1$  is the real part of the optical dielectric constant (i.e., the magnitude of  $\epsilon(q, \omega)$  at  $q = 0$ ). The stopping power can then be expressed from eq. (1) as

$$-\frac{dE}{ds} = \frac{4\pi N Z_{\text{eff}} e^4 \rho}{m_0 v^2 A} \ln \left[ \frac{m_0 v^2}{J_{\text{eff}}} \right] \quad (14)$$

where

$$Z_{\text{eff}} = \left[ \frac{2m_0}{h^2 e^2 n} \right] \int_0^E E' \cdot \text{Im} \left[ -\frac{1}{\epsilon(E')} \right] dE' \quad (15)$$

and

$$\ln(J_{\text{eff}}) = \left[ \frac{8\pi}{h^2 \omega_p^2} \right] \int_0^E E' \ln(E') \cdot \text{Im} \left[ -\frac{1}{\epsilon(E')} \right] dE' \quad (16)$$

where  $E'$  is the energy loss and

$$\omega_p^2 = \frac{4\pi e^2 n Z_{\text{eff}}}{m_0}$$

is the effective plasmon energy for the material.

In practice, unless the sample is very thin and the beam energy is high, the raw experimental energy loss spectrum  $I(E)$  is not identical to the single scattering distribution  $S(E)$ , but contains both plural and multiple scattering contributions. The single scattering spectrum can, however, be recovered by a suitable deconvolution procedure such as the logarithmic Fourier procedure due to Johnson and Spence (1974) or by an iterative method (Luo *et al.*, 1993). In the experiments described here, the experimental spectra were collected from a GATAN parallel electron energy loss spectrometer (PEELS), with an acceptance angle  $\alpha$  of between 5 and about 50 mrad, and an incident beam energy of 100 or 200 keV provided by a Philips EM400 field emission gun (FEG) transmission electron microscope (TEM) or an Hitachi H-800 TEM. Samples were prepared as thin foils by mechanical polishing and ion milling and typically had a thickness in the range 300-500 Å.

Spectra were obtainable over the energy loss range up to about 1 keV with acquisition times of from 2 to 20 seconds giving high enough counts per channel (typically greater than  $10^4$ ) to ensure a stable deconvolution result. The resolution of the spectrometer was about 1 eV and data was recorded for 1024 channels. Corrections for dark-current and DC offsets in the spectrometer and recording system were made using the procedures recommended by GATAN and were carried out before the spectra were stored for analysis. After Fourier deconvolution to extract the single scattering distribution, the energy loss function  $\text{Im} (-1/\epsilon)$  was obtained from the spectrum as discussed above and this was extrapolated to extend to an energy loss of several keV using values for  $\epsilon$  derived from mass absorption coefficient data (Hovington *et al.*, 1996). This is necessary to ensure that  $Z_{\text{eff}}$  and  $J_{\text{eff}}$  can be tracked until a sufficiently high energy so that they reach their expected maximum values of  $Z$  and  $J$ . Under some experimental conditions, it has been found that  $Z_{\text{eff}}$  does not always reach the

## Experimental Measurements of Electron Stopping Power at Low Energies

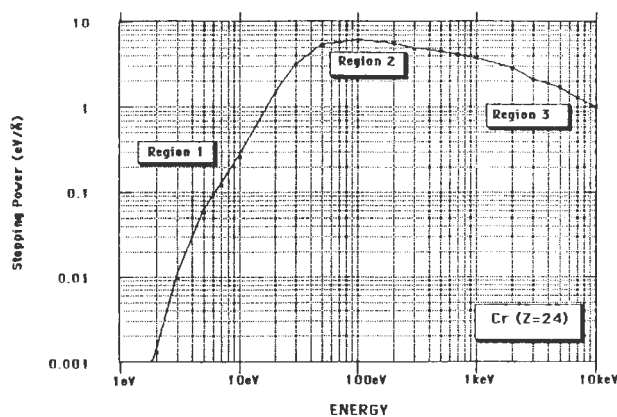


**Figure 1.** Experimentally determined variation of electron stopping power (in  $\text{eV}/\text{\AA}$ ) with energy for chromium (atomic number  $Z = 24$ ) from 1 eV to 10 keV.

anticipated  $Z$  value for the element; in these cases, a normalization is performed to bring it to the correct value.

### Experimental Results for Elements

The method described above has been used to determine the stopping power of a number of elements and some compounds. Figure 1 shows the experimentally determined variation of stopping power, plotted in units of electron volts per angstrom, as a function of electron energy for chromium (atomic number  $Z = 24$ ) over the range 1 eV to 10 keV. This data, both in its form and magnitude, is characteristic of all of the elements and compounds so far examined. The stopping power varies smoothly over a range of four orders of magnitude, starting from a very low value at electron energies below 10 eV, reaching a peak value of a few eV per angstrom at an energy of about 100 eV, and then falling monotonically at higher energies to a value of typically  $1.0 \text{ eV}/\text{\AA}$  at around 10 keV. For more detailed discussion, it is convenient to divide the data into three energy regions:

#### Region 1

In this region, covering energies from 1 eV up to about 30 eV (with the energy being referenced to the Fermi level of the specimen), the stopping power shows a steep rise with increasing energy  $E$  as shown in Figure 2 which compares the stopping power for carbon ( $Z = 6$ ), chromium ( $Z = 24$ ), palladium ( $Z = 46$ ), and lead ( $Z = 82$ ). For the very lowest energies, between 1 and about 10 eV above the Fermi level, the stopping power is generally extremely small (less than  $10^{-2} \text{ eV}/\text{\AA}$ ) and varies only slowly with energy. It must be noted, however, that when using the experimental procedures discussed here, it is difficult to obtain reliable data in this

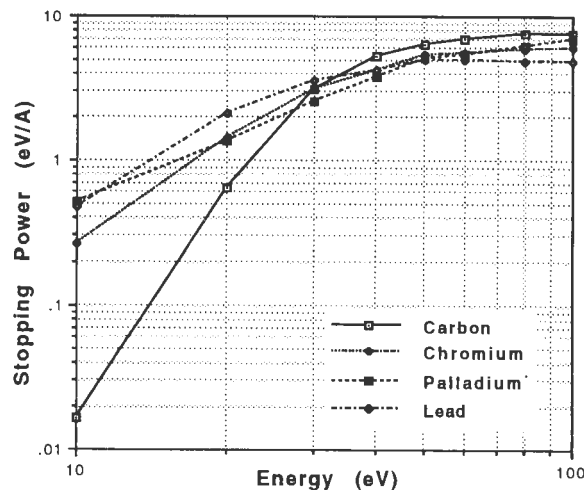


**Figure 2.** Experimental stopping power data (in  $\text{eV}/\text{\AA}$ ) in the low energy range (region 1) for carbon, chromium, palladium, and lead.

range because the limited energy resolution of the spectrometer and uncertainties in the position of the zero-loss scattering peak caused by electromagnetic interference result in the tail of the elastic peak being smeared over an energy range of 5 eV or more. Consequently, these values were treated with caution, and where optical data was available, this was used in preference. Once the incident electron energy exceeds 10 eV, which is typically the lowest ionization critical energy for an element, the stopping power starts to rise rapidly, varying with energy  $E$  as about  $E^n$  where  $n$  has been found to vary from a low value of 1.7 to a maximum value of 3. There is, at present, insufficient data to quantify the correlation between the magnitude of the exponent  $n$  and the atomic number of the specimen, but in general, the lower atomic number materials show a higher value of  $n$  than that found for higher  $Z$  specimens.

A general problem with the stopping power data retrieved in this energy range is in assessing the contribution of exchange effects. When exchange is considered, the simple relation between the dielectric function and the inelastic cross-sections assumed above is no longer valid, and consequently, the derived stopping power data may not be correct. However, recent first principles computations of stopping power using optical and photoelectric data (Fernandez-Varea *et al.*, 1993) and incorporating a modified Ochkur (1964) approximation for exchange interactions have produced profiles that agree closely with our experimental determinations as well as with other earlier calculations (see, for example, Ashley *et al.*, 1979; Tung *et al.*, 1979). Figure 3 compares our measured stopping power data for aluminum, silicon, copper, and gold in the energy range 10 eV to 0.3 keV, with the corresponding computed data of Fernandez-

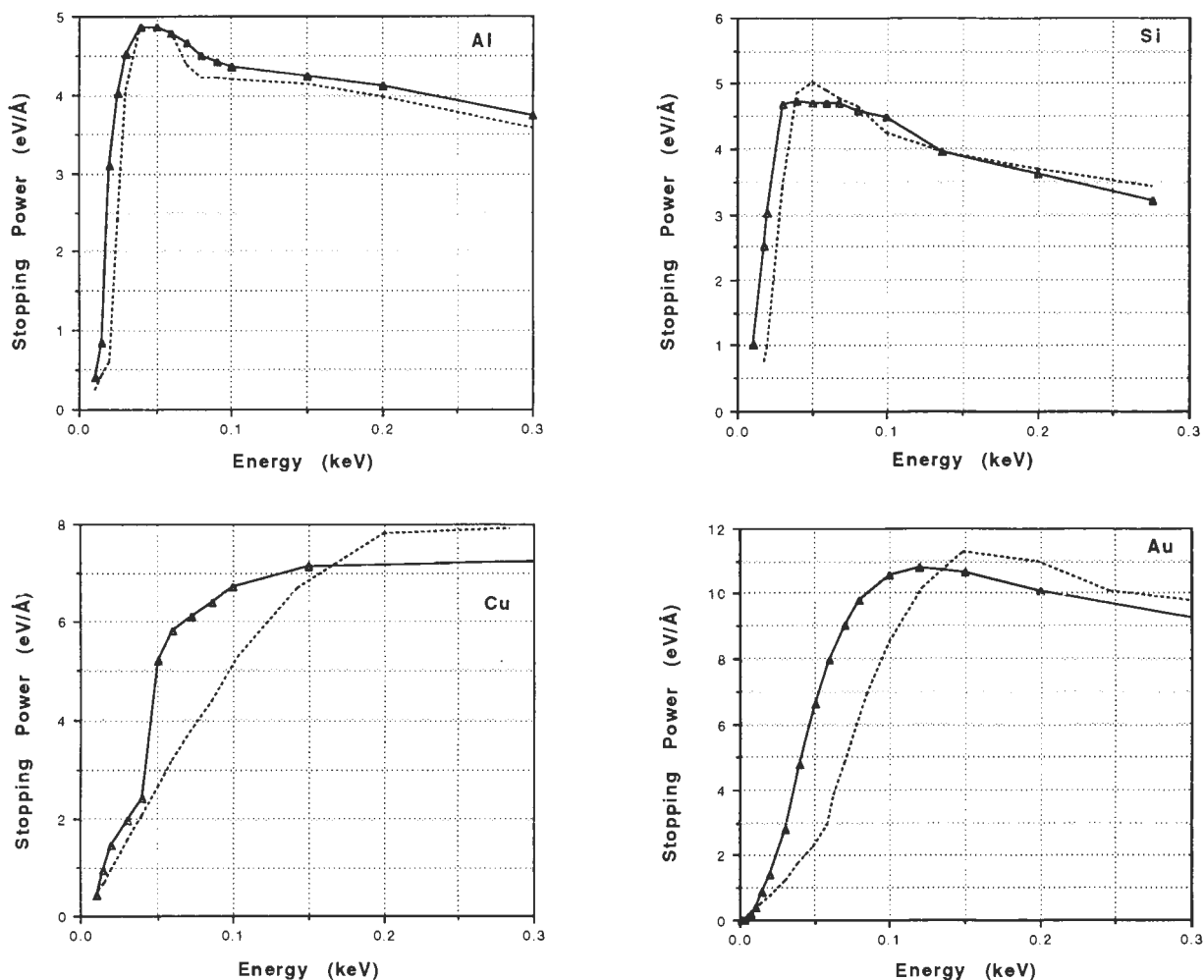


Figure 3. Experimental stopping power data (in eV/Å) in the low energy range for aluminum, silicon, copper, and gold, shown as solid lines and compared with the corresponding computed data of Fernandez-Varea et al. (1993) shown as dotted lines.

Varea *et al.* (1993). It can be seen that both the profile of the variation and the absolute magnitudes of the measured and calculated stopping power are generally in excellent agreement, although at some energies there is a discrepancy. Although these selected cases cannot prove that the method we have used gives results that are always correct, we believe it is an indication that the error due to exchange is probably small.

## Region 2

This region occurs at energies between 40 eV and 200 eV, depending on the material, and is where the stopping power reaches its maximum value, exhibits a plateau at which its magnitude is independent of the energy, and then begins to fall. The peak stopping powers measured for a number of different elements are plotted in Figure 4. For convenience, the data has been divided by the density of the target material to give the stopping power in units of MeV/g·cm<sup>2</sup>. A clear trend is evident with the peak stopping power falling steadily

as the atomic number increases. An estimate of the expected behavior can be made from the simple Bethe expression. Writing eq. (1) in the form

$$-\frac{dE}{\rho ds} = \frac{2\pi e^4 NZ}{AE} \ln \left[ \frac{1.166E}{J} \right] \quad (17)$$

and differentiating the stopping power with respect to E shows that the peak should occur when  $E = 2.33J$ . Inserting the values of the physical constants and using the Berger-Seltzer (1982) approximation that  $J \approx 9.76Z$  then gives the maximum stopping power  $SP_{\max}$  as occurring at energy  $E_{\max} = 22.75Z$  and having the value:

$$SP_{\max} = \frac{78500Z}{AE_{\max}} = \frac{3450}{A} \text{MeV/g}\cdot\text{cm}^2 \quad (18)$$

This relation is also plotted on Figure 4 for comparison

## Experimental Measurements of Electron Stopping Power at Low Energies

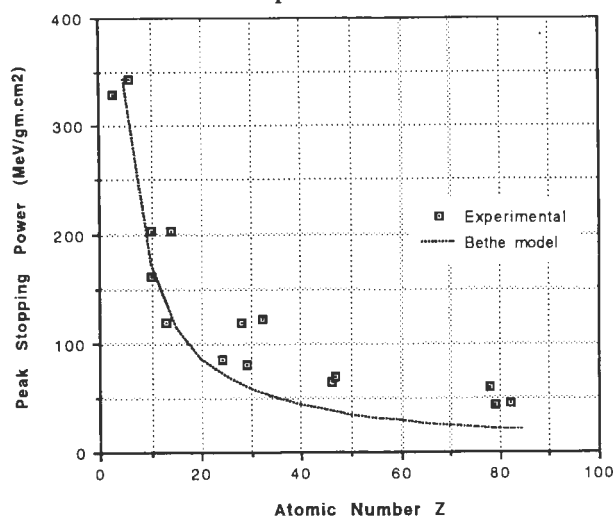


Figure 4. Experimentally determined peak stopping power in  $\text{MeV/g.cm}^2$  plotted as a function of atomic number for a variety of elements, and (solid line) a comparison with the values predicted by the Bethe equation.

and is seen to display the general trend of the experimental results, although usually lying lower in magnitude as might be expected since both  $Z_{\text{eff}}$  and  $J_{\text{eff}}$  are likely to differ substantially from their maximum values at this low energy. The correlation between the measured peak energies and the "predicted" value of  $22.75Z$  is much less obvious and indicates that other phenomena not included in the model, for example solid state effects, are playing a role.

### Region 3

In the third region, extending upwards in energy from the plateau, the stopping power falls monotonically with the energy, ultimately following the Bethe expression of eq. (1). This covers the energy range in which the majority of electron microscopy and microanalysis is performed, and is therefore the regime of major interest. Figure 5 shows our experimental data for aluminum in this regime and displays, in addition, independent measurements from five other groups. Considering the diversity of techniques employed to yield this data, the level of agreement between results is encouraging. Assuming that this agreement indicates that our techniques can safely be treated as reliable, even in the majority of those other cases for which there is no independent comparative data, a more detailed analysis can then be made of the stopping power behavior.

**The range of applicability of the Bethe law:** Because of its widespread use in the study of electron interactions, it is of interest to know the energy range over which the simplest form of the Bethe expression might be usable. If the values of  $N$  and  $J$  in eq. (1) are taken to be constant, then inserting the correct physical con-

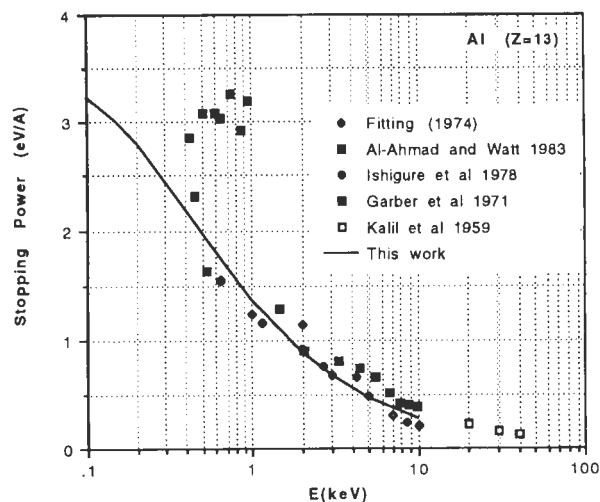


Figure 5. Comparison of experimentally measured stopping power for aluminum in region 2 and 3 from this work (solid line) and from other independent measurements.

stants and writing the stopping power relation as

$$-\frac{dE}{ds} = \frac{785 \rho Z}{AE} \ln \left( \frac{1.166 E}{J} \right) \quad (19)$$

implies that a plot of

$$Y = E \left[ -\frac{dE}{ds} \right] \left[ \frac{A}{785 \rho Z} \right]$$

vs.  $X = \ln(1.166E)$

will be a straight line when a Bethe-like relation is valid. An example of such a plot is shown in Figure 6. At high enough energies, an excellent straight line fit is indeed obtained. The utility of this plot is that the intercept of this line on the x-axis provides an estimate of the minimum energy at which Bethe-like behavior occurs. An analysis of all of the data so far obtained in this study, both for individual elements and for compounds, shows that the onset of the linear region occurs for an energy  $E_B$  such that  $\ln(1.166E_B/J)$  is greater than  $1.2 (\pm 0.05)$ . This corresponds to the condition  $E_B \geq (2.85 \pm 0.15)J$ , where the value of  $J$  is taken to be that given by the ICRU (1984) tables and implies, for example, that even for gold the unmodified Bethe law can probably be considered reliable down to about 2.5 keV. This estimate of the limiting energy  $E_B$  at which the Bethe relation is applicable is comparable to, but somewhat lower than, the value  $E_{RSW} \geq 6.4J$  suggested by Rao-Sahib and Wittry (1974), which corresponds to the position of the inflection of eq. (17).



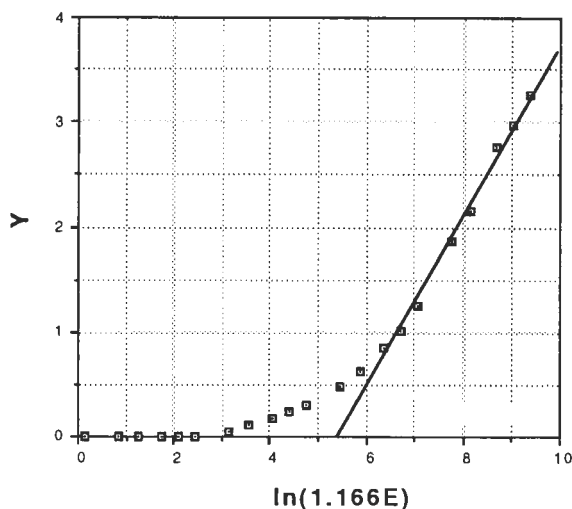


Figure 6. Plot to demonstrate range of applicability of a simple Bethe law relationship for germanium ( $Z=32$ ). The parameter  $Y$  is defined in the text.

Table 1. Comparison of measured and ICRU values of mean ionization potentials for elements and compounds.

Element/ compound	Z	Measured J (eV)	ICRU value (eV)
Carbon	6	69.5	76.0
Aluminum	13	164	166
Silicon	14	160	173
Chromium	24	250	257
Nickel	28	347	311
Copper	29	315	322
Germanium	32	345	350
Palladium	46	395	470
Silver	47	468	470
Platinum	78	725	790
Gold	79	898	823
Lead	82	898	823
-----			
Alumina ( $Al_2O_3$ )		135	145
Bismuth High Tc		530	
CuAu (50:50 alloy)		450	
GaAs		333	
GaSb		435	
Guanine		63	75
Ice		77	75
InSb		700	
MgO		122	
MoS <sub>2</sub>		223	
SiC		113	
SiO <sub>2</sub>		134	

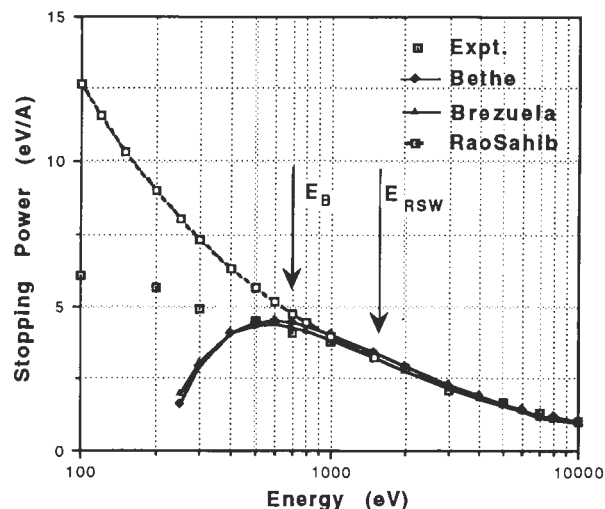


Figure 7. Replot of data of figure (1) for chromium but showing Bethe law (equation 1) fit for  $J=250$ eV. The suggested limiting values for the applicability of the Bethe relation,  $E_{RSW}$  and  $E_B$  are also shown. The corresponding predictions for the Brizuela and Riveros (1990) and Rao-Sahib Wittry (1974) relations are also shown for comparison.

#### Magnitude of the mean ionization potential $J$ :

The experimental data analysis procedure discussed earlier generates a value  $J_{eff}$  representing the effective applicable mean ionization potential at the given energy. As the energy  $E$  increases,  $J_{eff}$  tends asymptotically toward a limiting value  $J$  which can be compared with the standard tabulated ICRU (1984) figures as well as with the widely used Berger-Seltzer (1982) analytical fit. The limiting value of  $J$  can also be derived from the slope of the plot of eq. (19). Table 1 compares experimental limiting values of  $J$  with the corresponding ICRU values. In general, the agreement is seen to be close, but since  $J$  only appears inside a logarithmic term, its influence on the calculated absolute magnitude of the stopping power is limited in any case. A corollary of this result is that the ICRU mean ionization potential values can, when employed in eqs. (1) and (2), and within the limitations already discussed, accurately predict the stopping power for electron energies in the low keV region, even though they are derived from high energy experiments.

#### Compact Representations of the Stopping Power Data

For each of the materials so far analyzed, the stopping power data is available in tabular format (see note at the end of this paper for details) and so could be used directly, for example, in a Monte Carlo simulation (Hovington *et al.*, 1995). However, for use in Monte Carlo and other types of electron interaction models, it is often more convenient to be able to represent the data

analytically, since this minimizes the amount of data which must be stored and accessed during the operation of the program. The basis for any such model will be the Bethe relation, and Figure 7 replots the data of Figure 1 for chromium but superimposes on it the corresponding value predicted by eq. (1) using the  $J$  value obtained from the experimental data (c.f. Table 1). The suggested limiting energies discussed above,  $E_{RSW} = 6.4J$  and  $E_B \geq 2.85J$ , are also indicated on the figure for reference. As already noted, the Bethe relation is seen to predict a stopping power variation at high energies, which is very close in absolute magnitude and form to that determined experimentally, but as the energy falls towards the limiting values, the value predicted from eq. (1) diverges from those determined experimentally and ultimately goes to zero and changes sign.

The "failure" of the Bethe law at low energies is entirely predictable because in the form expressed by eq. (1), both  $N$  and  $J$  are treated as constants rather than as energy-dependent variables. If the correct experimental values of  $N_{eff}$  and  $J_{eff}$  at the energy of interest are used instead, then the stopping power predicted by eq. (1) remains close to that measured experimentally down to the lowest energies. While the Bethe equation has been employed in this form (e.g., Reimer and Stelter, 1986), there is little reduction in the amount of data that must be stored and it would seem to be more useful to use tabulated stopping powers directly.

The procedure of Livingstone and Bethe (1937), as adapted by Brizuela and Riveros (1990), uses different  $J_{eff}$  and  $Z_{eff}$  values above and below the K-edge critical energy  $E_K$ . Below  $E_K$ , the stopping power is determined by a single Bethe-like expression with the value  $Z_{eff}$  set to  $(Z - 1.81)$ , where  $Z$  is the atomic number of the target, and with a modified value of  $J_{eff} = J'$ . For over-voltages greater than 1.5 (i.e.,  $E > 1.5 E_K$ ), the stopping power is the sum of two terms, the one given above, and a second representing the contribution of the K-shell electrons only. Here,  $Z_{eff} = 1.81$  and  $J_K$  is given by

$$J_K = 15.0008(Z - 0.3)^2. \quad (20)$$

Brizuela and Riveros (1990) suggest that  $J'$ , the low over-voltage value of  $J$ , be calculated from the expression

$$J = (J')^{Z-1.81} (J_K)^{1.81}, \quad (21)$$

where  $J = 22.4Z^{0.828}$ . As shown in Figure 7, in which data for chromium are compared, this model behaves marginally better at low energies than the basic Bethe expression, since the maximum stopping power is slightly higher and the expression remains positive down to a lower energy. However, for chromium, the equation still becomes negative at an energy of only about 220 eV, so this expression is not useful for low energy

investigations. Although this modification is based on sound physical principles, and the evaluation of these expressions is straightforward, the improvement in accuracy that is achieved is minimal and does not seem sufficient to justify its adoption.

A common procedure has been to use the simple form of eq. (1) for high energies, but at lower energies, to use a parabolic extrapolation from the tangent to the Bethe curve at the energy  $E = 6.4J$ , where the curve has an inflection (Rao-Sahib and Wittry, 1974). Thus, for  $E < 6.4J$ , eq. (16) is replaced by the expression:

$$-\frac{dE}{ds} = \frac{62400Z}{\sqrt{EJA}} \quad (22)$$

As shown in Figure 7, this procedure produces a composite stopping power curve which has a somewhat closer resemblance to the experimental data over some of the low energy region, although the discrepancy between the actual and predicted values diverges rapidly as the energy falls and becomes unacceptably large for energies below about 100 eV. Although this expression satisfies the requirement for a compact representation of the data, this modification again has no physical basis and its poor accuracy makes it a less than ideal choice.

As noted earlier, the accuracy of the simple Bethe equation at low energies can be improved by modifying eq. (1) to the form given in eq. (2) (Joy and Luo, 1989), where  $k$  is a constant initially chosen to be 0.857 (i.e.,  $1/1.166$ ). At high energies, eq. (2) tends asymptotically to the standard Bethe expression eq. (1), but at low energies, the presence of the additional term in the numerator effectively makes  $J$  a function of  $E$ , since by comparing eqs. (1) and (2), we see that

$$J_{eff} = \frac{J}{1 + \frac{kJ}{E}} \quad (23)$$

As is the case with the original Bethe expression, the stopping power computed from eq. (2) can still go to zero and change sign as  $E$  is reduced, but this now occurs at an energy of  $J(0.857 - k)$  rather than at the energy  $0.857J$ , so the  $k$  parameter can be used to set the lower useful limit for the calculation of the stopping power if desired.

An appropriate value for  $k$  can be determined by iteratively fitting eq. (2) to the experimental data, and, in most cases, an excellent match to measured stopping power data can be obtained over a very wide energy range. Figure 8 compares the behavior of this expression for palladium where the parameter  $k = 0.807$ . It can be seen that over the energy range from 20 eV to 10 keV, the deviation between the fitted modified Bethe expression and the experimental data is typically less than

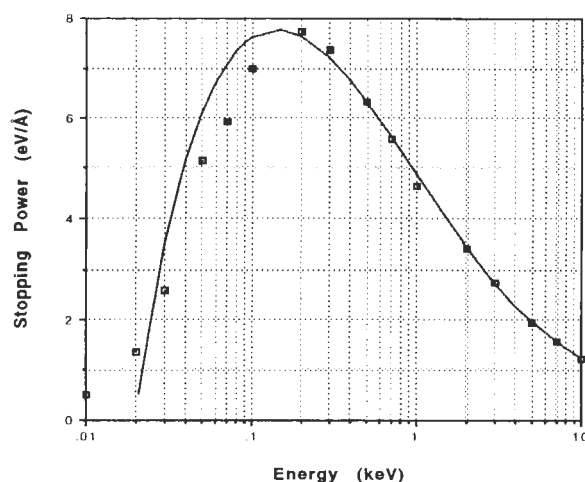


Figure 8. Experimental stopping data for palladium compared with modified Bethe model with  $k=0.8$

Table 2. Best fit  $k$ -value for modified Bethe expression.

Material	best fit value of $k$
carbon	0.570
aluminum	0.797
silicon	0.795
chromium	0.798
nickel	0.829
germanium	0.829
palladium	0.807
gold	0.832
lead	0.832
-----	
Bismuth Hi Tc	0.839
CuAu (50:50) alloy	0.843
GaAs	0.828
GaSb	0.828
Guanine	0.542
Ice	0.608
InSb	0.843
MgO	0.776
MoS <sub>2</sub>	0.786
sapphire	0.710
SiC	0.681
SiO <sub>2</sub>	0.708

10%, while, as demonstrated in Figure 7, the deviations for the other models can be as much as a factor of 3 times. Only at the lowest energies, where the experimental data is also of uncertain accuracy, is the error significant. Similarly good fits between this empirically modified Bethe expression and the experimental data has been found for about 75% of the elements so far measured. It must be noted, however, that for aluminum, germanium, and lead, the fit was less satisfactory, par-

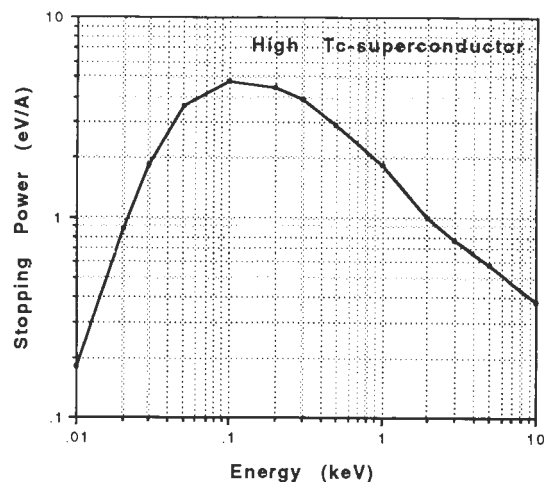


Figure 9. Experimental stopping power curve (in  $eV/\text{\AA}$ ) for a bismuth high  $T_c$  superconductor material.

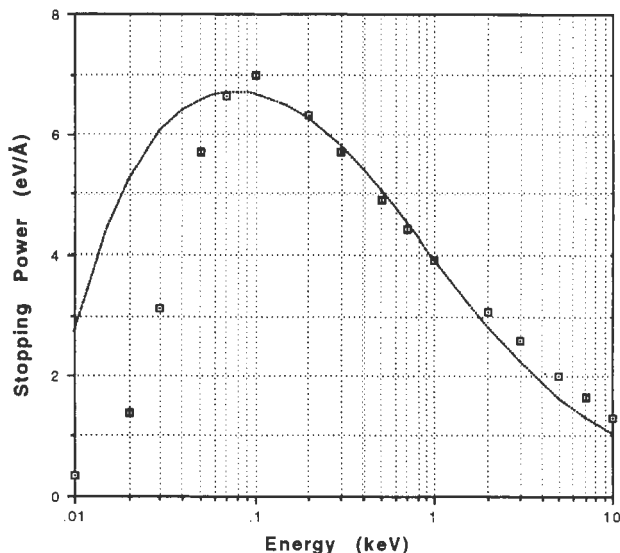
ticularly in the energy range between about 50 and 500 eV, although the fit was acceptable at high energies.

Table 2 lists the best fit  $k$ -values for the twelve elements so far measured. With the exception of the value for carbon, the numbers are quite close to the nominal value of 0.857 and to the values estimated by fitting eq. (2) to published first principles calculations of stopping power (Joy and Luo, 1989). The value of  $k$  appears to increase with atomic number, but there is, at present, insufficient data to quantify this variation. For any elements not so far measured, an estimate of the value of  $k$  in the range 0.82 to 0.85 should usually give a reasonable prediction of the stopping power over the energy range above about 500 eV.

The form of eq. (2), thus, so far appears to be the most convenient and compact way of representing the stopping power variation over the whole energy range. However, the variation of  $J$  with  $E$  generated by eq. (23) in no way matches the experimental variation of  $J_{\text{eff}}(E)$ , and the equation takes no account of the variation in  $Z_{\text{eff}}$ . Eq. (2) should therefore be properly regarded as an empirical, analytic fit and not a physical model.

### Experimental Results From Compounds

Stopping power curves have also been obtained for 15 or so compounds ranging from simple binary alloys to complex multi-element systems. As shown in Figure 9, which plots the data for a high critical-temperature superconducting alloy, the form of the stopping power variation is very similar to that for an individual element and exhibits the same three regimes of behavior: a sharp initial rise with energy, a plateau, and then a monotonic decay with a further increase in energy. The magnitude of the stopping power is of the same order as that for an individual element, and the high energy behavior follows



**Figure 10.** Experimental stopping power data (in eV/Å) for a 50:50 CuAu alloy (closed squares) showing the Joy-Luo (1989) modified Bethe fit with  $k=0.843$  (dotted line).

the conventional Bethe expression consistent with eq. (1). These parallels suggest that the strategy used to model the stopping power of elements may be equally applied to compounds.

The usual approach in microanalysis and Monte Carlo modeling has been to treat  $Z_{\text{eff}}$  as being the weighted average of the atoms present, and to derive a value for  $J_{\text{eff}}$  from the Berger and Seltzer (1982) relation. In many cases, this procedure works well, as is shown in Figure 10 which shows the experimental data for a 50:50 CuAu alloy and the corresponding fit using eq. (2) with  $J = 450$  eV and  $k = 0.843$ . The quality of the fit is good down to about 100 eV, but is worse at lower energies. Results as good as or better than this have been obtained for other compounds, including molybdenum di-sulfide  $\text{MoS}_2$ , silicon carbide  $\text{SiC}$ , and even for the complex nucleic acid guanine. However, this procedure has not been found as successful for materials such as sapphire ( $\text{Al}_2\text{O}_3$ ), possibly because of the large difference in atomic bonding between metallic aluminum and the ionic bonding in the sapphire, or for compound semiconductors ( $\text{GaAs}$ ,  $\text{InSb}$ , etc.), which show a significantly higher peak stopping power than expected from the modified Bethe equation. Table 1 lists the asymptotic limiting values of  $J$  as determined experimentally for some compounds. Table 2 shows the corresponding best-fit  $k$ -values for use in eq. (17).

An alternative and more rigorous approach is to treat the stopping power of the compound as the weighted sum of the stopping powers of its elemental constituents. As shown in Figure 11 with the data for CuAu, an

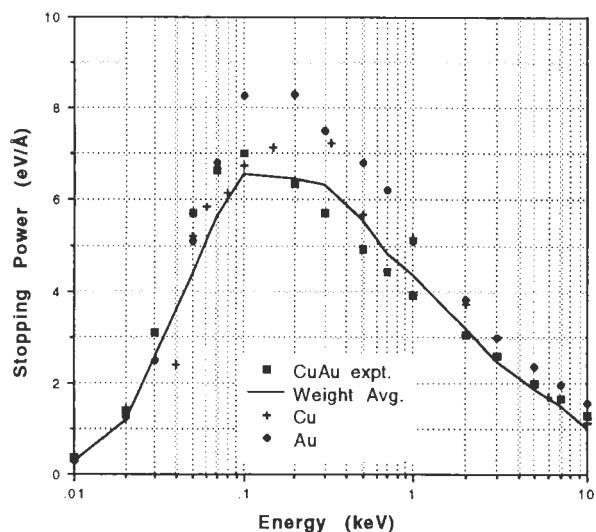


**Figure 11** The experimental data of figure (10) compared with the corresponding stopping powers for elemental Cu and Au, and with their weighted sum (dotted line).

excellent fit is then obtained over the entire energy range. The stopping power curves for gold and copper as pure elements have been added together using the weight fractions of the elements present to give the composite curve for the alloy. The fit to the experimental data from this procedure is better than that from the Bethe fit using the averaged  $Z$  and  $J$  values, especially at the lowest energies, although either could be used. It is noteworthy, however, that the mean ionization potential derived from the weighted averages for copper and gold in the CuAu alloy is 664 eV, which differs significantly from the "best fit" value of 450 eV determined using eq. (2). This again emphasizes that this modification to the Bethe expression must be treated as a fitting equation rather than as a physical model.

If the stopping power of a compound can generally be modeled as the weighted sum of the stopping powers of its constituents, then values can readily be determined for any compound once a full range of elemental stopping power data is available. While it can be expected that this procedure might be valid at high energies, it is possible that solid-state interactions might produce deviations at low energies. We have, therefore, set out to investigate this procedure by measuring stopping powers for binary compounds and comparing these data to the corresponding values from the elemental constituents. Data will be published as it becomes available.

### Conclusions

Electron stopping power data can be derived, over an energy range from a few electron volts up to an

energy of tens of keV, from electron energy loss spectra, optical spectra, and photon mass absorption data. The values derived show a generic behavior with stopping power rapidly increasing at low energies, reaching a plateau, and then monotonically decreasing at higher energies. Values deduced from the analysis are in good agreement with values predicted by first-principles theoretical models, and other independent measurements of stopping power. The behavior of compounds has been found to be similar to that of elements. The data so far available covers only a small fraction of the periodic table, and very few compounds, so a systematic program of study is still required to generate data to cover all the materials of interest to microscopists and microanalysts. Further work is also required to find convenient analytical representations of the stopping power profiles, since none of the models so far examined is fully satisfactory.

Copies of all the data so far analyzed can be obtained as either computer readable files or graphical plots from David Joy (see addresses on the first page of this paper).

#### Acknowledgements

This work was partially supported by an unrestricted grant from the Dow Chemical Co. USA, by the Government of Quebec under the Quebec-USA program for Scientific Collaboration, by the Division of Materials Sciences, U.S. Department of Energy under contract DE-AC05-84OR21400 with Lockheed Martin Energy Systems, Inc., and through the SHaRE program under contract DE-AC05-76OR00033 with Oak Ridge Associated Universities.

#### References

- Al-Ahmad KO, Watt DE (1983) Stopping powers and extrapolated ranges for electrons (1-10keV) in metals. *J. Phys. D: Appl. Phys.* **16**, 2257-61.
- Ashley JC (1988) Interaction of low-energy electrons with condensed matter: Stopping powers and inelastic mean free paths from optical data. *J. Electr. Spectros. and Rel. Phenomena* **46**, 199-214.
- Ashley JC, Tung CJ, Ritchie RH (1979) Electron inelastic mean free paths and energy losses in solids - 1 Aluminum, *Surf. Sci.* **81**, 409-426.
- Berger MJ, Seltzer SM (1982) Stopping Powers and Ranges of Electrons and Positrons (2nd edition) NBSIR 82-2550-A, 1-29.
- Bethe H (1930) Zur theorie des Durchganges schneller Korpuskularstrahlen durch Materie (Theory of the Passage of Fast Particle Beams Through Matter). *Ann. Phys.* **5**, 325-349.
- Brizuela H, Riveros J (1990) Study of mean excitation energy and K-shell effect for EPMA. *X-ray Spectrom.* **19**, 173-82.
- Daniels J, Festenberg CV, Raether H, Zeppenfeld K (1970) Optical constants of solids by electron spectroscopy. *Springer Tracts in Modern Physics* **54**, 77-99.
- Duncumb P, Da Casa C (1969) Improving quantitative X-ray microanalysis, Proc. 5th Int. Congress on X-ray Optics and Microanalysis. Mollenstedt G, Gaukler K (eds.). Springer, Berlin. pp. 146-151.
- Egerton RF (1996) *Electron Energy Loss Spectrometry*, 2nd Ed. Plenum Press, New York. pp. 123-44.
- Fernandez-Varea JM, Mayo R, Liljequist D, Salvat F (1993) Inelastic scattering of electrons in solids from a generalized oscillator strength model using optical and photoelectric data. *J. Phys: Condens. Matter* **5**, 3593-3610.
- Fitting H-J (1974) Transmission, energy distribution and SE excitation of fast electrons in thin solid films. *Phys. Stat. Sol. (a)* **26**, 525-35.
- Flinn EA, Salehi M (1980) The Fano plot in secondary electron emission studies, *J. Phys. D: Appl. Phys.* **13**, 1801-1809.
- Garber FW, Nakai MY, Harter JA, Birkhoff RD (1971) Low energy electron beam studies in thin aluminum foils. *J. Appl. Phys.* **42**, 1149-1158.
- Harrowfield IR, Cranswick LMD, Youl S (1994) Comparison of computed and measured bremsstrahlung spectra to test electron energy-loss models. *Microbeam Analysis* **3**, 161-175.
- Hovington P, Drouin D, Gauvin R, Joy DC, Luo S, Evans N (1995) Exploring the possibilities of low energy SEM with a specialized Monte Carlo program. In: *Microbeam Analysis 1995*. Etz E (ed.). VCH, New York. pp. 351-352.
- Hovington P, Drouin D, Gauvin R (1996) CASINO - a program for Monte Carlo simulation. *Scanning*, in press.
- ICRU (1984) Stopping Powers for Electrons and Positrons. Report #37 of the International Commission on Radiation Units, Bethesda, Maryland.
- Ishigure N, Mori C, Watanabe T (1978) Electron stopping power in aluminum in the energy region 2 to 10.9 keV. *J. Phys. Soc. Japan* **44**, 973-978.
- Johnson DW, Spence JCH (1974) Determination of the single-scattering probability distribution from plural-scattering data. *J. Phys. D: Appl. Phys.* **7**, 771-780.
- Joy DC (1995) A database on electron-solid interactions. *Scanning* **17**, 270-276. A copy of the complete database is available on request from the author.
- Joy DC, Luo S (1989) An empirical stopping power relationship for low-energy electrons. *Scanning* **11**, 176-180.
- Kalil F, Stone WG, Hubell HH, Birkhoff RD (1959) Stopping power of thin aluminum foils for 12 to 127 keV electrons. ORNL Report 2731. Oak Ridge National Lab., Oak Ridge, TN.

Livingstone H, Bethe H (1937) C - Nuclear Dynamics, *Experimental. Rev. Mod. Phys.* **9**, 245-379.

Luo S, Zhang X, Joy DC (1991) Experimental determinations of electron stopping powers at low energies. *Rad. Effects and Defects in Solids* **117**, 235-242.

Luo S, Dunlap JR, Joy DC (1993) Modulation electron energy loss spectroscopy and its application to quantitative analysis. *Proc. 51st Ann. Meeting MSA. San Francisco Press, San Francisco.* pp. 454-455.

Nieminen RM (1988) Stopping power for low energy electrons. *Scanning Microsc.* **2**, 1917-1926.

Ochkur VI (1964) The Born-Oppenheimer method in the theory of atomic collisions. *Sov. Phys. JETP* **18**, 503-508.

Pouchou J-L, Pichoir F (1987) Quantitative X-ray microanalysis. In: *X-ray optics and Microanalysis.* Brown J, Packwood R (eds.). University of Western Ontario. p. 249.

Rao-Sahib TS, Wittry DB (1974) X-ray continuum production from thick elemental targets for 10-50 keV electrons. *J. Appl. Phys.* **45**, 5060-5082.

Reimer L, Stelter D (1986) FORTRAN 77 Monte Carlo program for minicomputers using the Mott cross-section. *Scanning* **8**, 257-277.

Rez P, Glaisher RW (1991) Measurement of energy deposition in transmission electron microscopy. *Ultra-microscopy* **35**, 65-69.

Ritchie RH, Howie A (1977) Electron excitation and the optical potential in electron microscopy. *Phil. Mag.* **36**, 463-481.

Thompson JJ (1912) Ionization by moving electrified particles. *Phil. Mag.* **23**, 449-457.

Tung CJ, Ashley JC, Ritchie RH (1979) Electron inelastic mean free paths and energy losses in solids - II Electron Gas Statistical Model. *Surf. Sci.* **81**, 427-440.

### Discussion with Reviewers

**H.-J. Fitting:** In your eq. (16), the mean logarithm of the effective ionization energy is calculated without regard to the dispersion of  $\epsilon(q,E)$ . On the other hand, we know that even for low PE energies, the scattering with higher momentum transfer  $q$  increases. Is this reflected by the fitting-formula (eq. (2))? Should we understand eq. (2) as already averaging over  $q$ ?

**Authors:** It is true that there is a dispersion relation for  $\epsilon(q,\omega)$ . This is not explicitly considered in the theory because there is no convenient representation of the dispersion relationship that can be assumed for this purpose.  $J$  is therefore understood to be an average over  $q$ .

**P. Rez:** Do you think that other parameterizations (for example a set of two or three parabolas or cubics of the form  $a_0 + a_1E + a_2E^2 + a_3E^3$ ) might be more suitable than the Bethe expression in the low energy region?

**Authors:** It is very probable that parameterizations of this type might be better fits to the experimental data than the model used here over some specified energy range. However, the disadvantage of polynomial expressions is that their behavior outside of the fitting range may be very undesirable and this can lead to problems if such models are not used with caution. The advantage of the fit that we employed is that it has sensible behavior at both the high and low energy extremes.

**C.J. Powell:** You suggest that "solid state effects" might account for the poor correlation between the energy at which the stopping power is a maximum and the value  $22.75Z$  expected from the Bethe equation. The stopping power equation was originally derived by Bethe for atoms but is also applicable to solids. As the authors correctly point out, the Bethe equation is only expected to be valid for energies above some minimum revealed by a Fano plot such as that shown in Figure 7. Since the Bethe equation is not valid at lower energies, it is unlikely that the application of eq. (18) in this region would be useful other than to illustrate broad trends. Can the authors comment on this view?

**Authors:** Equation (18) was only intended to show the sort of trend that might be expected in the maximum stopping power data. As this maximum occurs at an energy which is lower than the experimentally determined limit of applicability of the Bethe equation, the values predicted by eq. (18) cannot necessarily be expected to be accurate. However, they do give a useful "rule of thumb" estimate of the maximum stopping power.

**C.J. Powell:** The authors have chosen to define the energy showing the onset of Bethe-like behavior in Figure 7 as the point where the extrapolated straight line intersects the abscissa axis (here about 220 eV). While this definition could be useful empirically, Figure 7 shows appreciable deviations of the experimental points from the fitted line at energies below about 500 eV. Since these two energy threshold differ by about a factor of two, would the authors wish to revise their definition?

**Authors:** The extrapolation of the straight-line region in Figure 7 gives an energy below which the Bethe equation cannot be used. Between that energy, and the inflection point at 6.4J suggested by Rao-Sahib and Wittry (1974) as a lower useful limit to the Bethe equation, the accuracy of the simple Bethe model falls. However, in simple applications, the stopping power predicted in this range is still at worst a plausible approximation and so can be of value. When higher accuracy is required, additional steps must be taken to improve the accuracy, and these are discussed in the text.

**C.J. Powell:** I was surprised by the authors' statement that a limiting value of  $J$  could also be derived, although with less precision, from the slope of plot of eq. 19

(Fig. 7). Please supply typical values of the precision for each type of determination. Please also supply numerical values for the average RMS differences between the sets of  $J$  values in Table 1. In the statement that eqs. (1) and (2) can "accurately predict the stopping power for electron energies in the low keV region even though they are derived from high energy experiments," please give an estimation of the likely degree of accuracy.

**Authors:** The choice of wording was, in retrospect, unfortunate. Determining  $J$  from the slope of the linear region Fano plot is straightforward. The "error" in this procedure derives from the necessity of deciding which points on the plot (e.g., Fig. 7) will not be included because they are below the energy at which linear behavior is expected. If only high energy values ( $E > 7J$ ) are included, there is no difficulty; if lower energy values are fitted, then the addition or removal of one data point can have a significant ( $\approx \pm 10\%$ ) effect on the value of  $\ln(J)$ , and hence a fairly major effect on the value of  $J$  itself. Values of  $J$  derived by optimizing the fit of the entire stopping power curve to eq. (2) are less sensitive to the choice of data points. We did not quote RMS deviations for our data because we do not believe that we presently have sufficient data sets to make a reliable judgement.

**R.F. Egerton:** How do we know that energy  $E$  is relative to the Fermi level?

**Authors:** Our assumption was that we could take the reference energy for "free" electrons as being the Fermi level. This is not an assertion that this is actually the case, although the error is probably small.

**R.F. Egerton:** Why is it more rigorous to add stopping power rather than the effective number of electrons contributed by different elements in a compound?

**Authors:** The addition of stopping powers allows variations in both  $N_{\text{eff}}$  and  $J_{\text{eff}}$  to be considered. This is necessary because  $N_{\text{eff}}$  and  $J_{\text{eff}}$  both change with energy.

**M. Kotera:** The stopping power is defined by eq. (8) using the inelastic scattering cross-section of the primary electron. This value inherently ignores events which occur after the collision. For example, in the electron head-on collision to a stationary free-electron, the primary electron stops, but the scattered SE moves with the same energy as the PE before the collision. Do you think that the contribution of SE generated can be taken into account as an effective value of the stopping power, or can this contribution be ignored?

**Authors:** The way in which the concept of stopping power is formulated considers only the PE and this does not make it possible to incorporate the other effects that you mention that also contribute to the transfer of energy to the material. Those effects are accounted for in the actual values of  $N_{\text{eff}}$  and  $J_{\text{eff}}$  which must be used to fit the experimental stopping power measurements.

**M. Kotera:** The number of effective atomic electrons can be obtained by using the equation below eq. (16) in a comparison between this equation and the experimentally determined plasmon energy. How do you think of this relationship if the experimental plasmon energy has a wide distribution, as is usually observed for transition elements?

**Authors:** It is true that the upper limit of  $N_{\text{eff}}$  could, in principle, be determined from experimental measurements of plasmon losses. The practical difficulty, as you point out, is that the plasmon peak has a finite width. This comes from the functional form of the complex dielectric function of the material and is physically related to the fact that the electrons are not really "free," i.e., they have an effective mass which differs from that of a single isolated electron, and because there is a dispersion relationship coupling the plasmon energy to the momentum transfer in the inelastic scattering event. Equation (16) is a simplified expression intended only to illustrate the physical relevance of these parameters.

**M. Kotera:** It is easy to calculate the electron range from this stopping power. If there is some experimental results of the electron range, it would be informative to compare calculated and the experimental values.

**Authors:** The range that can be computed directly from the stopping power data is usually called the Bethe or CSDA (continuous slowing down approximation) range and is the average distance that an electron must travel in a given material to give up some specified fraction of its initial energy. It is not easy to compare CSDA ranges with values determined from electron transmission and scattering data, since such measurements depend also on the nature and amount of elastic scattering that occurs in the experimental geometry that was employed. While the different range estimates are clearly related, the form of the relationship changes with energy and with the target material and can only be properly examined through Monte Carlo simulation methods.

**I. Harrowfield:** Prof. L. Reimer did a relativistic version of this formula. Should that be used for higher energies (e.g., 10 keV and above)?

**Authors:** At energies high enough for relativistic effects to become significant (typically 100 keV and above), additional interactions must be included in the Bethe model. A variety of formalisms have been suggested to do this including the Reimer model that you mention, and many others. All of these high energy expressions simplify to, or asymptotically approach, the conventional Bethe equation at low energies, but diverge from it at higher energies. One or another of these forms should certainly be used for electron energies in excess of 100 keV since they all suggest that the stopping power falls more slowly at high energies than the  $1/E$  variation implied by the Bethe model.